Transversal flexoelectric coefficient for nanostructures at finite deformations from first principles

David Codony, Irene Arias, and Phanish Suryanarayana

Phys. Rev. Materials **5**, L030801 — Published 8 March 2021

DOI: 10.1103/PhysRevMaterials.5.L030801

Transversal flexoelectric coefficient for nanostructures at finite deformations from first principles

David Codony,[1] Irene Arias,[1,2] and Phanish Suryanarayana[3,*]

[1] *Laboratori de Càlcul Numèric, Universitat Politècnica de Catalunya, Barcelona, E-08034, Spain*
[2] *Centre Internacional de Mètodes Numèrics en Enginyeria (CIMNE), 08034 Barcelona, Spain*
[3] *College of Engineering, Georgia Institute of Technology, Atlanta, GA 30332, USA*

(Dated: February 23, 2021)

We present a novel formulation for calculating the transversal flexoelectric coefficient of nanostructures at finite deformations from first principles. Specifically, we introduce the concept of *radial polarization* to make the coefficient a well-defined quantity for uniform bending deformations. We use the framework to calculate the flexoelectric coefficient for group IV atomic monolayers using density functional theory. We find that graphene's coefficient is significantly larger than previously reported, with a charge transfer mechanism that differs from other members of its group.

Introduction. Flexoelectricity [1–7] is an electromechanical property common to insulating systems that represents a two-way coupling between strain gradients and polarization. In contrast to piezoelectricity, it is not restricted to materials with a specific symmetry, and in contrast to electrostriction, it permits reversal of the strain by reversal of the electric field. Due to the possibility of large strain gradients, the flexoelectric effect is particularly significant in nanostructures, making them ideal candidates for a number of applications, including energy harvesting, sensing and actuating.

A fundamental obstacle in characterizing and exploiting the flexoelectric effect is the significant disagreement between theory and experiment, with coefficients differing by up to three orders of magnitude, and sometimes even in the sign [2, 3, 8]. In view of this, perturbative approaches in the framework of Kohn-Sham density functional theory (DFT) [9] have been developed for calculating the flexoelectric tensor components from first principles [10–15]. However, the coefficients so computed, of which the transversal component μ_{T} is particularly important for nanostructures, correspond to the asymptotic zero strain gradient limit. Therefore, they are restricted to linear response, likely not representative at the relatively large curvatures commonly encountered in experimental investigations involving bending deformations [16–19].

Kohn-Sham DFT calculations for μ_{T} at finite bending curvatures are perhaps simpler than their zero-curvature counterparts, since perturbation theory can be circumvented [20–22]. However, as illustrated in Fig. 1, a fundamental issue in this context is that μ_{T} becomes an ill-defined quantity on employing the standard definition of polarization. In particular, considering a structure that is extended in the X_1-direction, the value for μ_{T} is dependent on the choice of the unit cell in that direction. In fact, in the limiting case of the deformed unit cell encompassing the complete circle, $\mu_{\mathrm{T}} = 0$ for any charge distribution, a result that is clearly incorrect. Even for structures that are finite along the X_1-direction, μ_{T} has an artificial dependence—not attributable to edge-related effects—on the corresponding dimension of the structure, i.e., on the angle subtended by the bent structure. Note that the calculation of μ_{T} requires only the transversal component of the polarization, which can be determined without the need for the Berry phase formulation, since the structure is finite along this direction, with the corresponding reciprocal lattice vector being orthogonal to the reciprocal lattice vectors associated with the extended directions.

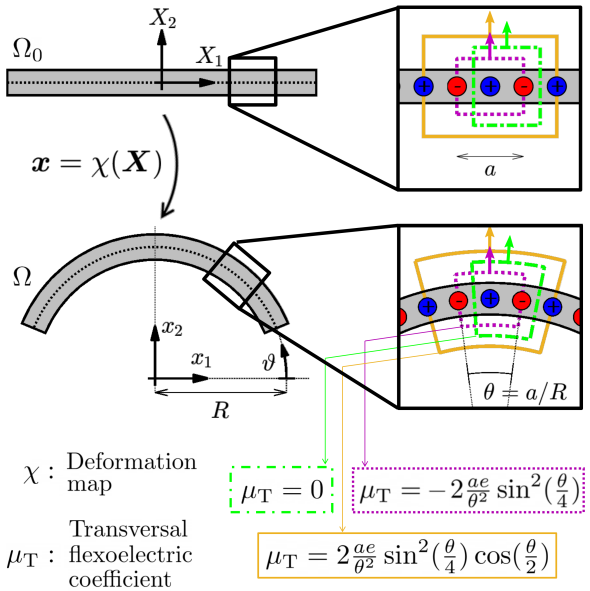

FIG. 1. Illustration depicting the ill-defined nature of the transversal flexoelectric coefficient when the standard definition for the polarization is employed for a structure that is extended in the X_1-direction. The arrows indicate the component of polarization that needs to be computed.

In this work, we introduce the concept of *radial polarization* to overcome the ill-defined nature of transversal flexoelectric coefficient μ_{T} at finite bending deformations. In particular, we show that μ_{T} is naturally defined in terms of the radial polarization at large deformations,

which is the setting for a number of experimental [16–19] and theoretical studies [20–22]. Indeed, this definition reduces to the standard one in the zero strain gradient limit. We then use this formulation to calculate μ_{T} for group IV atomic monolayers along both the armchair and zigzag directions from ab initio DFT simulations.

Formulation. Consider a deformation $\boldsymbol{x} = \boldsymbol{\chi}(\boldsymbol{X})$, where the map $\boldsymbol{\chi} : \Omega_0 \mapsto \Omega$ transforms a point with coordinates $\boldsymbol{X} = [X_1, X_2, X_3]^{\mathrm{T}}$ in the undeformed configuration Ω_0 to the coordinates $\boldsymbol{x} = [x_1, x_2, x_3]^{\mathrm{T}}$ in the deformed configuration Ω. The associated deformation gradient tensor $\mathbf{F}(\boldsymbol{X})$ is defined as $F_{iI} := \partial\chi_i/\partial X_I$, whose Jacobian $J := \det(\mathbf{F})$. The corresponding Green-Lagrange strain gradient tensor $\mathbf{G}(\boldsymbol{X})$ is defined as $G_{IJK} := \frac{1}{2}\partial\left(F_{kI}F_{kJ}\right)/\partial X_K$, where the repeated index implies summation, a notation adopted henceforth. In this finite-deformation setting, the polarization $\boldsymbol{p}(\boldsymbol{x})$ can be expressed as [23]:

$$p_l = \left(\epsilon_0\chi_{\mathrm{e}}E_L + \mu_{LIJK}G_{IJK}\right)F^{-1}_{Ll}\,, \tag{1}$$

where the electric field $\boldsymbol{E}(\boldsymbol{X})$ is defined as the negative gradient of the electrostatic potential in the undeformed configuration, and $\boldsymbol{\mu}$ the fourth-order (form II) bulk flexoelectric tensor. It can therefore be inferred that:

$$\mu_{LIJK} = \left.\frac{\partial\left(p_lF_{lL}\right)}{\partial G_{IJK}}\right|_{\boldsymbol{E}}. \tag{2}$$

The above definition, which suggests that the flexoelectric tensor is the rate of change of $(\boldsymbol{p}\cdot\mathbf{F})$ with respect to the strain gradients, represents a key departure from literature. In particular, though previous non-perturbative works employ configurations that essentially correspond to finite bending deformations [20–22], they neglect the contribution from the deformation gradient $\mathbf{F}$, which causes the aforedescribed ill-defined nature of the transversal flexoelectric coefficient. The need for the deformation gradient becomes apparent by noticing that the polarization field is over the deformed configuration, whereas the flexoelectric tensor must be defined in the undeformed one [23]. The definition in Eq. 2 also differs from that proposed in curvilinear coordinates [24, 25], where the rate of change of $(J\mathbf{F}^{-1}\cdot\boldsymbol{p})$ with respect to strain gradients is instead considered. While this definition is *a priori* correct, the one proposed here is more convenient since the computation of the geometrical term suggested in Refs. [24, 25] is not required. Moreover, results from follow-up work [26] for systems not studied here are in significantly better agreement with experiments than other theoretical predictions [21, 25], suggesting the practical applicability of the proposed definition.

Though the definition in Eq. 2 is valid for any arbitrary deformation, we restrict ourselves to pure bending deformations, since they are sufficient to characterize the transversal flexoelectric coefficient, as shown below. On identifying Ω_0 with a slab in the X_1-X_3 plane and with some thickness in the X_2 direction (Fig. 1), pure bending around the X_3 axis can be represented using the deformation:

$$\begin{bmatrix}x_1\\x_2\\x_3\end{bmatrix} = \boldsymbol{\chi}\left(\begin{bmatrix}X_1\\X_2\\X_3\end{bmatrix}\right) = \begin{bmatrix}(R+X_2)\cos\vartheta\\(R+X_2)\sin\vartheta\\\lambda_3X_3\end{bmatrix}, \tag{3}$$

where R is the radius of curvature, $\vartheta = \pi/2 - X_1/R$, and λ_3 is the axial stretch. The deformation gradient and strain gradient tensors then take the form:

$$\mathbf{F} = \begin{bmatrix}+(J/\lambda_3)\sin\vartheta & \cos\vartheta & 0\\ -(J/\lambda_3)\cos\vartheta & \sin\vartheta & 0\\ 0 & 0 & \lambda_3\end{bmatrix}, \tag{4}$$

$$\mathbf{G} = \frac{J}{\lambda_3}\left[\begin{bmatrix}0&0&0\\0&0&0\\0&0&0\end{bmatrix}\begin{bmatrix}1/R&0&0\\0&0&0\\0&0&0\end{bmatrix}\begin{bmatrix}0&0&0\\0&0&0\\0&0&0\end{bmatrix}\right], \tag{5}$$

where $J/\lambda_3 = (1 + X_2/R) \approx 1$, assuming that R is large relative to the thickness of the system, which generally holds true for nanostructures. The only component of $\mathbf{G}$ that does not vanish is $G_{112} \approx 1/R = \kappa$, where κ is the curvature. It therefore follows from Eq. 2 that the transverse flexoelectric coefficient $\mu_{\mathrm{T}} := \mu_{2112} = \partial\left(p_lF_{l2}\right)/\partial\kappa$, which can be rewritten using Eq. 4 as:

$$\mu_{\mathrm{T}} = \frac{\partial\left(\boldsymbol{p}\cdot\boldsymbol{n}\right)}{\partial\kappa} = \frac{\partial p_r}{\partial\kappa}, \tag{6}$$

where $p_r := \boldsymbol{p}\cdot\boldsymbol{n}$ is defined to be the *radial polarization*, with $\boldsymbol{n} = [\cos(\vartheta), \sin(\vartheta), 0]^{\mathrm{T}}$ representing the unit vector normal to the uniformly bent structure.

The above formulation reveals the fundamental difference between the standard and proposed definitions for the transverse flexoelectric coefficient μ_{T}. Specifically, the current work suggests that μ_{T} is the rate at which the radial polarization p_r changes with curvature [27], instead of the x_2-component of the polarization, as assumed previously [20, 21]. In particular, the definition presented here can be viewed as a generalization of the standard one to finite bending deformations, agreeing in the limit $\kappa \to 0$. Indeed, the proposed formulation is applicable even to the nonlinear regime, overcoming a key limitation of the standard definition.

In electronic structure calculations such as DFT, the radial polarization takes the form:

$$p_r = \frac{1}{\|\Omega\|}\int_\Omega (r - R^{\mathrm{eff}})\rho(\boldsymbol{x})\ \mathrm{d}\Omega, \tag{7}$$

where $\|\Omega\|$ denotes the volume of Ω, and the integral can be interpreted as the *radial dipole moment*. Specifically, $r := \boldsymbol{x}\cdot\boldsymbol{n} = R + X_2$ signifies the radial component of $\boldsymbol{x}$, $R^{\mathrm{eff}} = \boldsymbol{X}^{\mathrm{eff}}\cdot\boldsymbol{n} = R + X_2^{\mathrm{eff}}$ is the *radial centroid* of the ions, with $\boldsymbol{X}^{\mathrm{eff}}$ being the centroid of the ions relative to the undeformed configuration, and ρ is the electron density. In obtaining the above expression, it has been

assumed that the total (i.e., electrons+ions) density is charge neutral, thereby also ensuring the invariance with respect to translations of the coordinate system. Note that p_r and therefore μ_{T} are independent of the choice of unit cell for structures extended in the X_1-direction, and do not display an artificial dependence on the corresponding width for finite structures, thereby overcoming a fundamental limitation of the standard definition.

Interestingly, the radial polarization takes the following form in the undeformed configuration:

$$p_r = \frac{1}{\|\Omega\|} \int_{\Omega_0} (X_2 - X_2^{\mathrm{eff}}) \rho_0(\boldsymbol{X}) \, \mathrm{d}\Omega_0, \tag{8}$$

where $\rho_0 = J\rho$ is the nominal electron density. Therefore, the radial dipole moment in the deformed configuration Ω corresponds to the standard dipole moment along the X_2-direction in the undeformed configuration Ω_0, confirming the Lagrangian nature of the flexoelectricity tensor $\boldsymbol{\mu}$ [23].

Implementation. The calculation of the transversal flexoelectric coefficient μ_{T} requires the derivative of the radial polarization p_r with respect to curvature κ, the direct evaluation of which necessitates the use of density functional perturbation theory (DFPT) [28, 29]. Given the complexities and challenges associated with such an approach, we instead employ a numerical approximation for the derivative, which requires computing p_r at multiple curvatures in the vicinity of the curvature κ at which μ_{T} is desired.

The proposed formulation for p_r is not restricted by the solution scheme for the Kohn-Sham problem, including the choice of coordinate system. It is however desirable for the chosen approach to efficiently simulate bending deformations commensurate with those found in experiments [16–19]. Given the large system sizes encountered, for extended structures in particular, ab initio simulation of bending deformations is particularly challenging, even with state-of-the-art DFT codes [30–32]. This is because DFT calculations are highly expensive, scaling cubically with system size and possessing a large prefactor, particularly when systematically improvable discretizations are used.

The calculation of p_r for structures that are extended in the X_1-direction requires that edge-related effects be avoided. One option is to consider a large enough structure in this direction, and use the nearsightedness principle [33, 34] to restrict the evaluation of p_r from Eq. 7 to a unit cell sufficiently far from the edges. A simpler and significantly more efficient alternative, which is employed in this work, is to instead consider the complete circle for the deformed structure and exploit the cyclic symmetry present in the system [35–37], as illustrated in Fig. 2.

The cyclic symmetry-adapted method reduces the computations to the unit cell in the angular direction—analogous to the periodic unit cell for translational symmetry—while solving the Kohn-Sham equations in cylindrical coordinates using the real-space finite-difference method [30, 38]. In so doing, the computational cost scales linearly with radius of curvature, enabling tremendous savings, particularly considering the highly parallelizable nature of such calculations. This makes it the ideal tool for the study of the flexoelectric effect [36, 37, 39]. Note that standard periodic boundary conditions are employed along the x_3-direction to account for the translational symmetry in that direction.

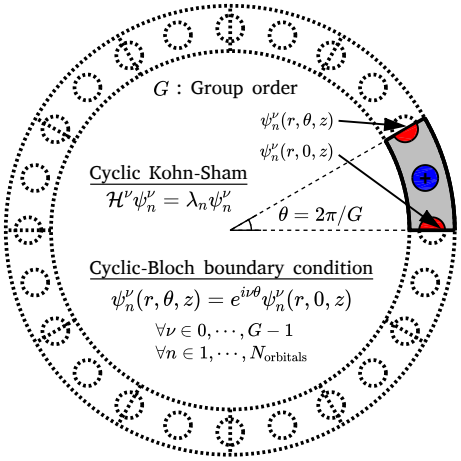

FIG. 2. Overview of the cyclic symmetry-adapted formulation for the Kohn-Sham eigenproblem [36, 37]. The Hamiltonian and Kohn-Sham orbitals are denoted by $\mathcal{H}^\nu$ and ψ_n^ν, respectively.

Results and discussion. We compute the transversal flexoelectric coefficient μ_{T} in both armchair and zigzag directions for the group IV atomic monolayers: graphene, silicene, germanene, and stanene. This is done for two choices of exchange-correlation functional: local density approximation (LDA) [40] and Perdew-Burke-Ernzerhof (PBE) [41] generalized gradient approximation (GGA). Optimized norm-conserving Vanderbilt (ONCV) pseudopotentials [42, 43] are employed, whose transferability for the chosen systems has been verified by ensuring that the equilibrium monolayer structures—determined using the planewave DFT code ABINIT [44]—are in good agreement with literature [45, 46]. Curvatures of $\kappa \sim 0.19 - 0.75$ nm^{-1} are considered, representative of those encountered in practice [16–19]. Structural and atomic relaxations are performed, ensuring that the final configuration corresponds to a pure bending deformation. All numerical parameters are chosen so that the μ_{T} are computed with an accuracy of $0.01e$. Additional information regarding the simulations and the accuracy of the results presented below can be found in the Supplementary Material.

The variation of radial polarization with curvature for the group IV monolayers is presented in Fig. 3, and the corresponding values for μ_{T} are listed in Table I. Due to the disagreement in literature over the thick-

ness of atomic monolayers [47], the radial dipole moments are normalized with respect to the area instead of volume while computing the radial polarization using Eq. 7, i.e., the units of μ_T here are $[e]$, rather than the conventionally used $[e/\text{bohr}]$. In addition, the dipole moments/polarization are calculated using the standard sign convention used in ab initio calculations, i.e., electrons are positive and ions are negative, which makes the sign of the reported flexoelectric coefficients opposite of continuum theories. Note that a single curvature-independent value is listed for each entry in the table since the flexoelectric coefficients have been found to be essentially constant for the bending deformations considered here, signaling linear response for the chosen curvatures. Therefore, the values of μ_T reported here can also be interpreted as those corresponding to the asymptotic limit of $\kappa \to 0$.

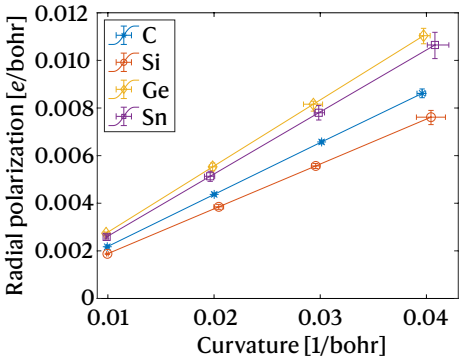

FIG. 3. Radial polarization p_r as a function of curvature κ for the group IV atomic monolayers. The error bars are used to denote variations corresponding to the different bending directions (i.e., zigzag and armchair) and exchange-correlation functionals (i.e., LDA and PBE).

	Zigzag		Armchair	
	LDA	PBE	LDA	PBE
Graphene	0.22	0.22	0.22	0.22
Silicene	0.19	0.19	0.19	0.19
Germanene	0.28	0.28	0.28	0.27
Stanene	0.27	0.26	0.27	0.26

TABLE I. Transversal flexoelectric coefficient μ_T $[e]$ for group IV atomic monolayers.

Notably, the results for the atomic monolayers studied in this work are independent of the exchange-correlation functional, the key approximation within DFT. In addition, the nearly identical values in the zigzag and armchair directions indicate that group IV monolayers are transversely isotropic with regards to flexoelectricity. The flexoelectric coefficients between the different materials are comparable, with germanene/stanene having the largest value ($\mu_T \sim 0.27e$), silicene having the smallest ($\mu_T \sim 0.19e$), and graphene towards the lower end ($\mu_T = 0.22e$).

The value for graphene is twice as large as that reported by Ref. [20], also computed using DFT, but with the standard definition of polarization. To confirm that this is not a consequence of edge-related effects that are absent in our calculations, in Fig. 4, we present μ_T as a function of the angle subtended by graphene strips of different widths, as computed using the different formulations, i.e., standard polarization, radial polarization, and atomic dipole model [22]. The results for the radial polarization and atomic dipole clearly indicate that edge effects are negligible. Interestingly, the standard polarization results in values for μ_T that are opposite to those reported here and in other theoretical works [22, 25]. This can be attributed to the the standard definition of the flexoelectric coefficient having an artificial dependence on the width, as discussed previously. Note that the value for μ_T computed using the atomic dipole model, which is in good agreement with that reported previously using this method [22], is more than two times smaller than the value predicted here. This is a consequence of the atomic dipole model requiring an artificial partitioning of the electron density within DFT. It is worth noting that though these results cannot be compared with experiments due to lack of data for the monolayers studied here, our follow-up work for other monolayers [26] demonstrates that the proposed formulation has significantly better agreement with experiments than other theoretical works [21, 25].

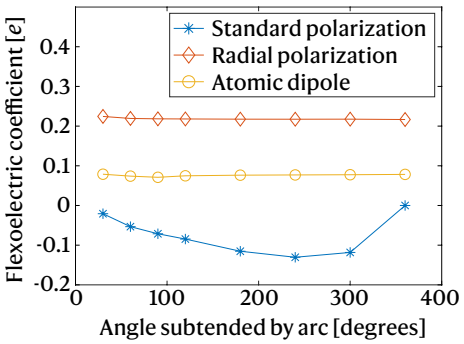

FIG. 4. Variation in flexoelectric coefficient μ_T as a function of the angle subtended by graphene strips of different widths subject to a bending deformation with curvature $\kappa = 0.04$ bohr^{-1}, as computed by the different formulations.

A comparison of the flexoelectric coefficients for atomic monolayers with their bulk counterparts is likely to provide fundamental insights into the effect of the dimensionality of the system on this material property. However, a systematic comparison is hindered by the lack of a well-defined thickness for the 2D materials [47]. If we were to assume a thickness of 10 bohr — commensurate with the typical out-of-plane extent of atomic orbitals — the corresponding flexoelectric coefficients for graphene and silicene would be 0.022 and 0.019 e/bohr,

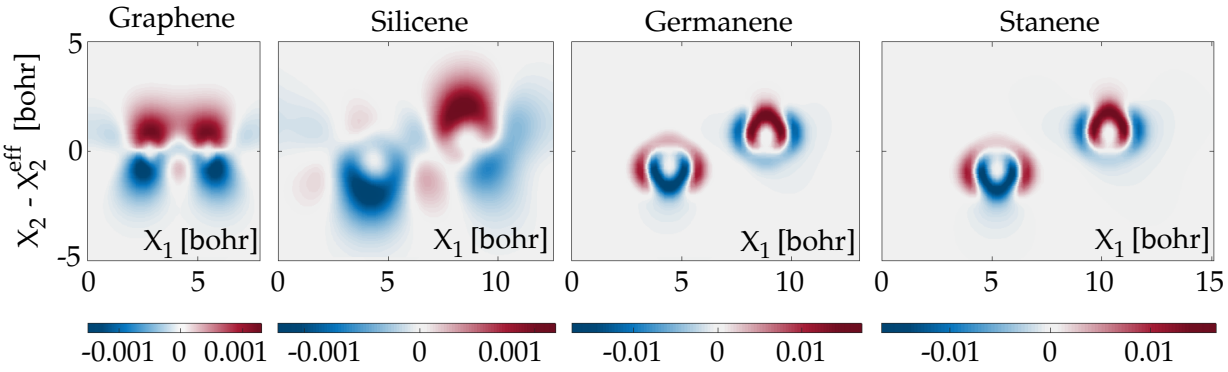

FIG. 5. Contours of nominal electron density difference (e/bohr^3) between the armchair bent ($\kappa = 0.19$ nm^{-1}) and flat atomic monolayers. The contours are in the $X_1 - X_2$ plane passing through the two fundamental atoms.

respectively, while the values for their bulk counterparts, i.e., graphite and silicon, have been reported to be 0.10 and 0.13 e/bohr, respectively [12]. Indeed, the structural thickness so defined can differ from the effective thickness of the monolayer [47]. In particular, the effective thickness can be many fold smaller, which would translate to comparable values for the flexoelectric coefficients of monolayers and their bulk counterparts.

To get insights into the underlying nature of the flexoelectric effect for the chosen monolayers, we plot in Fig. 5 the nominal electronic charge redistribution on the $X_1 - X_2$ plane passing through the two fundamental atoms. For all materials, there is a net radial charge transfer that occurs from below the neutral axis to above it. However, the plots indicate that there is a fundamental difference between graphene and the other members in its group. For graphene, bending introduces an asymmetry in the p-orbital overlap, leading to a rehybridization from sp^2 to some intermediate state between sp^2 and sp^3 [22, 48, 49]. However, the charge transfer in the other monolayers occurs between the two atoms and not due to the rehybridization of the orbitals within each atom.

Concluding remarks. In summary, we have presented a novel formulation for calculating the transversal flexoelectric coefficient of nanostructures at finite deformations from first principles. Specifically, we have introduced the concept of *radial polarization* to redefine the flexoelectric coefficient, making it a well-defined quantity for uniform bending deformations. The proposed framework has been used to calculate the coefficients for group IV atomic monolayers using DFT simulations. We have found that graphene's flexoelectric coefficient is significantly larger than that reported previously, with a charge transfer mechanism that fundamentally differs from the other members of its group.

The framework developed here is general and not restricted to the linear response of atomic monolayers. Therefore, it can be used to compute the transversal flexoelectric coefficients for interesting and more complex systems, including multilayer materials such as ferroelectric perovskites, making it a worthy subject for future research. Additionally, by considering deformations other than pure bending, the framework can be extended to compute other components of the flexoelectric tensor, making it another worthy subject for future research.

Acknowledgments. This work was supported in part by the Generalitat de Catalunya (ICREA Academia award for excellence in research to I.A., and Grant No. 2017-SGR-1278), and the European Research Council (StG-679451 to I.A.). I.A. acknowledges financial support from the Spanish Ministry of Economy and Competitiveness, through the "Severo Ochoa Programme for Centres of Excellence in R&D" (CEX2018-000797-S). P.S. gratefully acknowledges the support of the U.S. National Science Foundation (CAREER-1553212). The authors acknowledge discussions with Shashikant Kumar and his help with some simulations. P.S. acknowledges discussions with Amartya Banerjee prior to starting this work. The authors also acknowledge the valuable comments of the anonymous referees.

* phanish.suryanarayana@ce.gatech.edu

[1] A. K. Tagantsev, Phase Transit. **35**, 119 (1991).
[2] P. Yudin and A. Tagantsev, Nanotechnology **24**, 432001 (2013).
[3] P. Zubko, G. Catalan, and A. K. Tagantsev, Annu. Rev. Mater. Sci. **43** (2013).
[4] T. D. Nguyen, S. Mao, Y.-W. Yeh, P. K. Purohit, and M. C. McAlpine, Adv. Mat. **25**, 946 (2013).
[5] F. Ahmadpoor and P. Sharma, Nanoscale **7**, 16555 (2015).
[6] S. Krichen and P. Sharma, J. Appl. Mech. **83** (2016).
[7] B. Wang, Y. Gu, S. Zhang, and L.-Q. Chen, Prog. Mater. Sci. **106**, 100570 (2019).
[8] J. Hong, G. Catalan, J. Scott, and E. Artacho, J. Phys. Condens. Matter. **22**, 112201 (2010).
[9] W. Kohn and L. J. Sham, Phys. Rev. **140**, A1133 (1965).
[10] R. Resta, Physical review letters **105**, 127601 (2010).
[11] J. Hong and D. Vanderbilt, Phys. Rev. B **84**, 180101(R) (2011).

[12] J. Hong and D. Vanderbilt, Phys. Rev. B **88**, 174107 (2013).
[13] M. Stengel, Phys. Rev. B **88**, 174106 (2013).
[14] M. Stengel, Phys. Rev. B **90**, 201112(R) (2014).
[15] C. E. Dreyer, M. Stengel, and D. Vanderbilt, Phys. Rev. B **98**, 075153 (2018).
[16] N. Lindahl, D. Midtvedt, J. Svensson, O. A. Nerushev, N. Lindvall, A. Isacsson, and E. E. Campbell, Nano Lett. **12**, 3526 (2012).
[17] X. Chen, C. Yi, and C. Ke, Appl. Phys. Lett. **106**, 101907 (2015).
[18] W. Qu, S. Bagchi, X. Chen, H. B. Chew, and C. Ke, J. Phys. D **52**, 465301 (2019).
[19] E. Han, J. Yu, E. Annevelink, J. Son, D. A. Kang, K. Watanabe, T. Taniguchi, E. Ertekin, P. Y. Huang, and A. M. van der Zande, Nat. Mater. , 1 (2019).
[20] S. V. Kalinin and V. Meunier, Phys. Rev. B **77**, 033403 (2008).
[21] W. Shi, Y. Guo, Z. Zhang, and W. Guo, J. Phys. Chem. Lett. **9**, 6841 (2018).
[22] T. Dumitrică, C. M. Landis, and B. I. Yakobson, Chem. Phys. Lett. **360**, 182 (2002).
[23] D. Codony, P. Gupta, O. Marco, and I. Arias, J. Mech. Phys. Solids **146**, 104182 (2021).
[24] M. Stengel, Nat. Commun. **4**, 1 (2013).
[25] M. Springolo, M. Royo, and M. Stengel, arXiv preprint arXiv:2010.08470 (2020).
[26] S. Kumar, D. Codony, I. Arias, and P. Suryanarayana, Nanoscale **13**, 1600 (2021).
[27] The definition is in agreement with reduced models for flexoelectric membranes [5].
[28] X. Gonze and C. Lee, Phys. Rev. B **55**, 10355 (1997).
[29] S. Baroni, S. De Gironcoli, A. Dal Corso, and P. Giannozzi, Rev. Mod. Phys. **73**, 515 (2001).
[30] Q. Xu, A. Sharma, B. Comer, H. Huang, E. Chow, A. J. Medford, J. E. Pask, and P. Suryanarayana, arXiv preprint arXiv:2005.10431 (2020).
[31] A. S. Banerjee, L. Lin, P. Suryanarayana, C. Yang, and J. E. Pask, J. Chem. Theory Comput. **14**, 2930 (2018).
[32] P. Motamarri, S. Das, S. Rudraraju, K. Ghosh, D. Davydov, and V. Gavini, Comput. Phys. Commun. **246**, 106853 (2020).
[33] E. Prodan and W. Kohn, Proc. Natl. Acad. Sci. U. S. A. **102**, 11635 (2005).
[34] P. Suryanarayana, Chem. Phys. Lett. **679**, 146 (2017).
[35] A. Sharma and P. Suryanarayana, Phys. Rev. B **103**, 035101 (2021).
[36] S. Ghosh, A. S. Banerjee, and P. Suryanarayana, Phys. Rev. B **100**, 125143 (2019).
[37] A. S. Banerjee and P. Suryanarayana, J. Mech. Phys. Solids **96**, 605 (2016).
[38] Q. Xu, A. Sharma, and P. Suryanarayana, SoftwareX **11**, 100423 (2020).
[39] A. S. Banerjee, *Density Functional Methods for Objective Structures: Theory and Simulation Schemes*, Ph.D. thesis, University of Minnesota, Minneapolis, Minneapolis, MN (2013).
[40] J. P. Perdew and Y. Wang, Phys. Rev. B **45**, 13244 (1992).
[41] J. P. Perdew, K. Burke, and M. Ernzerhof, Phys. Rev. Lett. **77**, 3865 (1996).
[42] D. R. Hamann, Phys. Rev. B **88**, 085117 (2013).
[43] M. Schlipf and F. Gygi, Comput. Phys. Commun. **196**, 36 (2015).
[44] X. Gonze, B. Amadon, G. Antonius, F. Arnardi, L. Baguet, J.-M. Beuken, J. Bieder, F. Bottin, J. Bouchet, E. Bousquet, *et al.*, Comput. Phys. Commun. **248**, 107042 (2020).
[45] K. S. Novoselov, D. Jiang, F. Schedin, T. J. Booth, V. V. Khotkevich, S. V. Morozov, and A. K. Geim, Proc. Natl. Acad. Sci. U.S.A. **102**, 10451 (2005).
[46] S. Balendhran, S. Walia, H. Nili, S. Sriram, and M. Bhaskaran, Small **11**, 640 (2015).
[47] Y. Huang, J. Wu, and K.-C. Hwang, Phys. Rev. B **74**, 245413 (2006).
[48] I. Nikiforov, E. Dontsova, R. D. James, and T. Dumitrică, Phys. Rev. B **89**, 155437 (2014).
[49] S. Kundalwal, S. Meguid, and G. Weng, Carbon **117**, 462 (2017).